

## CHARACTERISATION OF ELM TRIGGERED EDGE PRESSURE CYCLES IN JET

J Lingertat, K Borrass<sup>\*</sup>, G D Conway, M Gould, K Günther, L D Horton,  
G F Matthews, V Parail, G Saibene

*JET Joint Undertaking, Abingdon, Oxon, OX14 3EA, UK*

*\*Max-Planck-Institut für Plasmaphysik, Garching, Germany*

### 1. Introduction

Recently a detailed study [1,2,3,4] has been made in JET of the scaling of the critical edge pressure,  $p_{up}$ , at which ELMs are triggered. A complete description of the edge pressure cycle during an ELM additionally requires an analysis of both the drop of the edge pressure  $\delta p$  during an ELM, and the recovery time  $\tau$  of the edge pressure. This paper focuses on the scaling of  $\delta p$ .  $\delta p$  is directly related to the stored energy loss per ELM  $\delta W$ , which in turn controls the maximum thermal load onto the divertor target plates. Knowledge of the scaling of  $\delta p$  is essential for extrapolation to future devices such as ITER.

### 2. Experimental

We have analysed neutral beam heated, steady-state ELMy H-mode discharges in the MkIIa and MkIIGB divertor configurations. The edge pressure  $p(t)$  was obtained from measured values of the edge electron density  $n(t)$ , and electron temperature  $T(t)$ . Assuming  $n_e = n_i$ ,  $T_e = T_i$  then  $p(t) = 2n(t)T(t)$ . The edge density was measured by interferometry at a major radius  $R = 3.75$  m ( $R_0 \sim 3$  m), the edge temperature profile by ECE. The stored energy  $W(t)$  was obtained from diamagnetic loop measurements. The main variation of  $T$  was achieved by varying the gas fuelling rate from discharge to discharge. Other parameters were varied between  $B_t = 2.7 - 3.5$  T,  $I_p = 2 - 3.7$  MA,  $P_{in} = 8 - 15$  MW,  $q_{95} = 2.4 - 4.5$  and the triangularity between  $\delta_{upper} = 0.18 - 0.43$ . Fig. 1 shows a sequence of discharges of a gas fuelling scan. Fig. 2 shows examples of  $W(t)$  and  $p(t)$ .

The data analysis was performed using values of  $T$ ,  $n$ ,  $p$  and  $W$ , just before an ELM ( $T_{up}$ ,  $n_{up}$ ,  $p_{up}$ ,  $W_{up}$ ), and just after an ELM ( $T_{low}$ ,  $n_{low}$ ,  $p_{low}$ ,  $W_{low}$ ), and by fitting an exponential function between two ELMs (Fig. 3). For each discharge the ELM parameters were averaged over  $\sim 10 - 30$  ELMs. A principal problem in the analysis is that  $\delta p (= p_{up} - p_{low})$  and  $\delta W (= W_{up} - W_{low})$  are each the difference between two large numbers (see fig. 2), giving large error bars.

### 3. Scaling

Fig.4 shows that  $\delta W$  is proportional to  $\delta p$ , from which we infer that the scaling results obtained for  $\delta p$  are valid also for  $\delta W$ . An analysis of the relative contribution of the plasma core and pedestal to  $\delta W$ , using the same procedure as in [2], shows that  $\delta W$  is mainly caused by a drop of the pedestal stored energy.

In the absence of a complete physics model of the pressure drop during an ELM, one has to speculate about the parameters that control  $\delta p$ . Tentatively, we adopt two different approaches: Firstly, we try to scale  $\delta p$  against the edge parameters  $p_{up}$ ,  $T_{up}$  and  $S_{95}$  and the global parameter  $I_p$ , implicitly assuming that  $\delta p$  is controlled by MHD physics. Secondly, we separately scale  $p_{up}$  and  $p_{low}$ , using for  $p_{up}$  the results of Refs [1,2,3,4]. For  $p_{low}$  we consider two alternative models. Model 1 assumes  $p_{low}$  is controlled by the same parameters as  $\delta p$  (MHD physics), whereas model 2 assumes that scrape-off layer physics largely controls  $p_{low}$

and implies  $n_{low}$ ,  $P_{SOL}$ ,  $B_t$  and  $q_\psi$  to be the relevant variables [5]. In fact model 2 combines empirical results on typical profile shapes in the pedestal and near separatrix region with the scaling relations provided by scrape-off layer physics. The units used in the following scaling equations are in MA, eV and  $10^{19} \text{ m}^{-3}$ , T, MW.

The first approach (fig. 5) gives as a scaling relation  $\delta p = 5.08 \cdot 10^{-5} I_p^{2.3} T_{up}^{2.3} n_{up}^{-0.6} S_{95}^{0.25}$ . This agrees qualitatively with the experimental observation of an increasing  $\delta p$  with pedestal temperature and plasma current and a decreasing  $\delta p$  with pedestal density. However, the dependence on  $I_p$  and  $T_{up}$  seems to be rather strong. The scaling relation can formally be written in terms of the local variables  $\rho_{pol} \propto \sqrt{T_{up}} I_p^{-1}$ ,  $\nu \propto n_{up} T_{up}^{-2}$  and  $\beta_{pol} \propto \rho_{up} I_p^{-2}$ , where  $\rho_{pol}$  is the poloidal Larmor radius,  $\nu$  the collisionality and  $\beta_{pol}$  the poloidal beta. The resulting scaling equation is  $\delta p / p \propto \rho_{pol}^{-1.6} \nu^{-1.2} \beta_{pol}^{-0.4} S_{95}^{0.25}$ . It does not contain geometrical variables and is therefore not applicable to other devices.

The second approach starts with the analysis of  $p_{up}$ . Here it is assumed that  $\rho_{up} \propto I_p S^2 T^{0.5}$ , which is well established for gas fuelled discharges in JET [2,3]. It is related to the ballooning limit of a pressure gradient over a transport barrier of width  $\rho_{pol}$ . Fig. 6 shows the scaling result. Data from discharges with type III ELMs are clearly separated and were not used in the fitting procedure.

The scaling of  $p_{low}$  using models 1 and 2 is shown in fig. 7 and 8, respectively. In model 1 only data obtained in type I ELM discharges are included. In model 2, both type I and type III data are used, because under the made assumption for model 2 (SOL physics controls  $p_{low}$ ), the result should be independent of the ELM type. With the scaling expressions obtained for  $p_{up}$  and  $p_{low}$ ,  $\delta p$  can be calculated. For model 1 a simple expression for the relative pressure drop can be derived  $\delta p / p = 1 - 2.2 n_{up}^{0.4} T_{up}^{-0.2} I_p^{-0.4}$ , which shows a weak dependence of the relative pressure drop on the selected parameters. This can be transformed into the dimensionless form  $\delta p / p = 1 - const. (\nu \beta_{pol})^{0.2}$ . Model 2 does not allow a further simplification of the scaling relation, because the variables used to scale  $p_{up}$  and  $p_{low}$  are not compatible.

#### 4. Summary

Scaling expressions for the edge pressure drop  $\delta p$  during ELMs have been derived for NB heated ELM H-mode discharges in JET. The three models tested describe within the error bars the data equally well. Since  $\delta p$  is shown to be proportional to the loss of stored energy  $\delta W$  these relations can be used to scale  $\delta W$ . The lack of a physics model for the pressure drop limits the application of the scaling expressions to the JET experiment. An extrapolation to larger devices requires the inclusion of geometrical parameters. This can only be achieved by comparing the JET results in a second step with results obtained on smaller devices.

- [1] J Lingertat et al., J. Nucl. Mater. 266-269 (1999) 124.
- [2] J G Cordey "H-mode power threshold and confinement in JET H, D, D-T and T plasmas" IAEA-F1-CN69/Ex7/1, paper presented at 17<sup>th</sup> IAEA Fusion Energy Conf., Yokohama, 1998.
- [3] G Saibene et al. "The influence of isotope mass, edge magnetic shear and input power on high density ELM H-modes in JET" submitted to Nucl. Fusion.
- [4] V P Bhatnagar et al., Nucl. Fusion 39 (1999) 235.
- [5] K Borrass, J Lingertat, J Schweinzer, in preparation

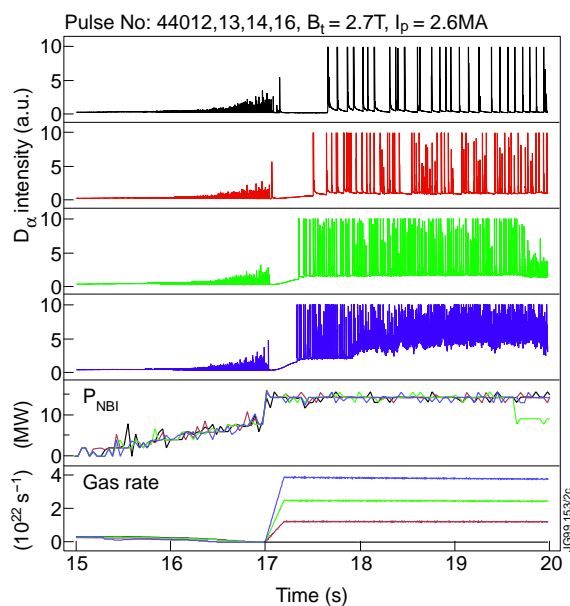


Fig. 1 Typical sequence of NB heated H-mode discharges in a gas fuelling scan

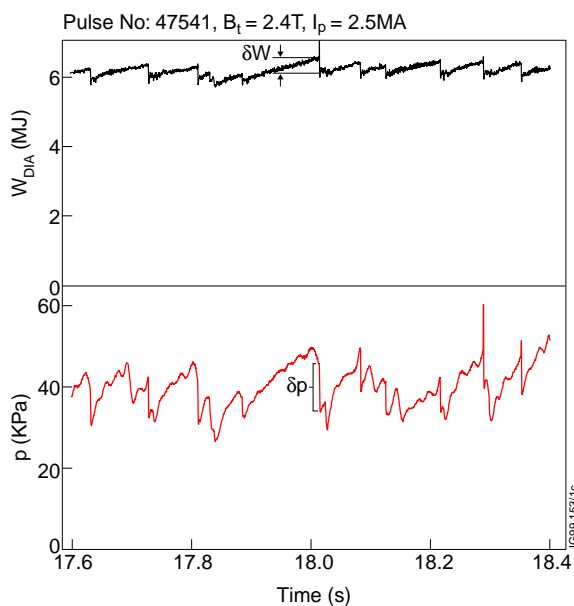


Fig. 2 Time traces of the diamagnetic energy and the edge pressure

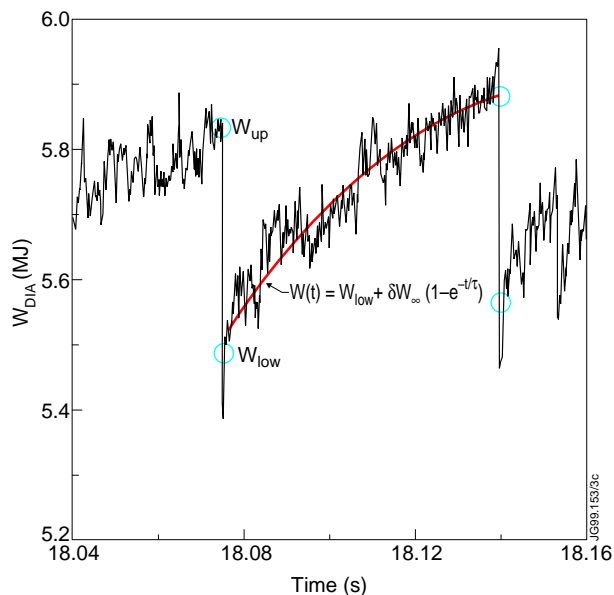


Fig. 3 Fitting parameters of the time evolution of the diamagnetic energy between two ELMs

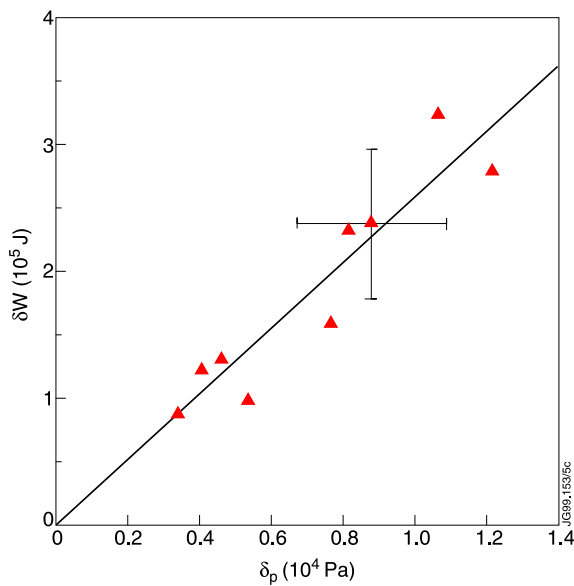


Fig. 4 Proportionality between  $\delta W$  and  $\delta p$

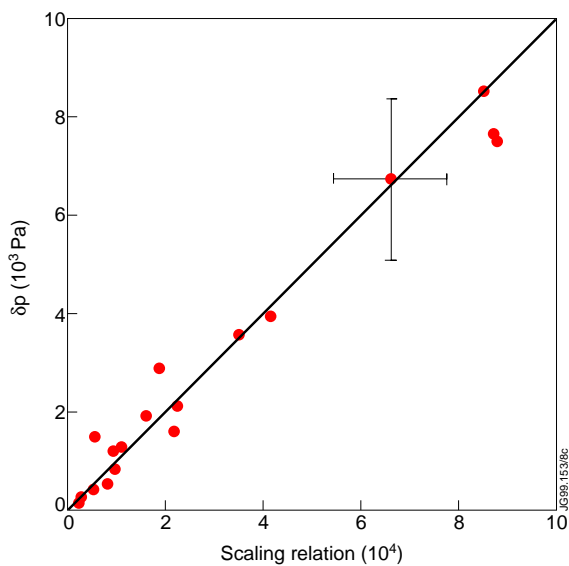


Fig.5 Scaling of the pressure drop.  

$$\delta p = 7.7 \cdot 10^{-5} p_{up}^{-0.6} I_p^{2.3} T_{up}^{2.9} S_{95}^{0.25}$$

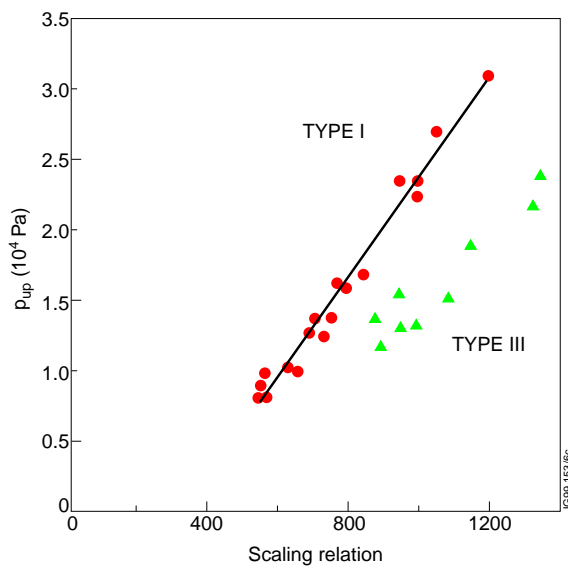


Fig.6 Scaling of the upper pedestal pressure.  

$$p_{up} = 17.6 I_p S_{95}^2 T_{up}^{0.5} - 5750$$

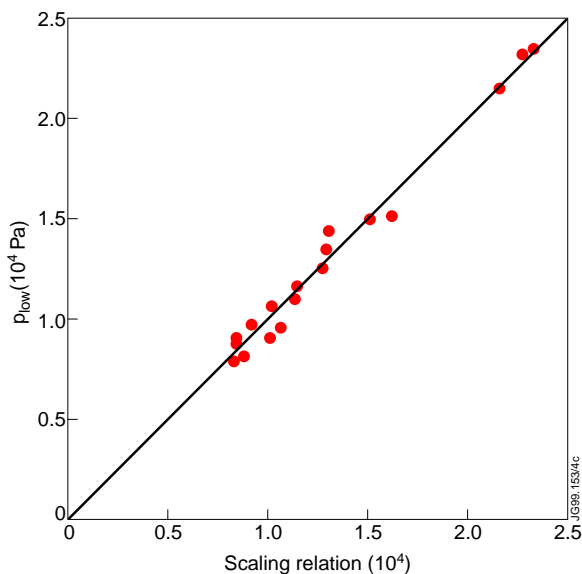


Fig.7 Scaling of the lower pedestal pressure, model 1.  

$$p_{low} = 4.4 p_{up}^{1.4} I_p^{-0.4} T_{up}^{-0.6}$$

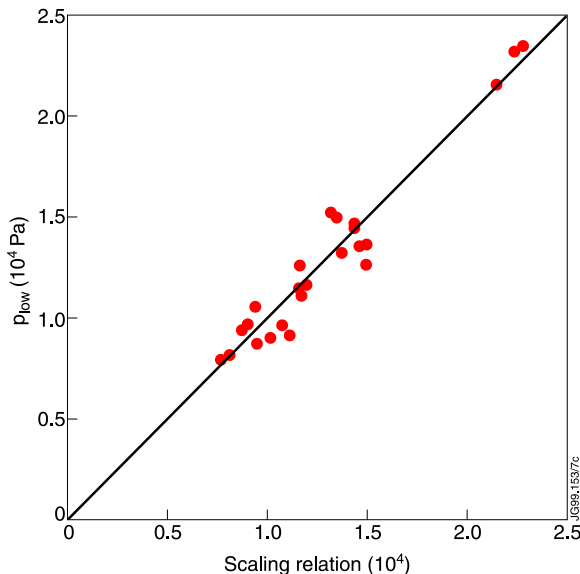


Fig.8 Scaling of the lower pedestal pressure, model 2.  

$$p_{low} = 2.56 \cdot 10^3 n_{low}^{0.22} P_{SOL}^{0.67} B_t^{0.91} q_{\psi}^{-0.69} - 2720$$